Electronic Supplementary Material (ESI) for ChemComm.

Supporting Information

In-situ grown high-valence Mo doped NiCo Prussian blue analogue for enhanced urea electrooxidation

Xiaoxing Zhou,[a,b] Jun Hu,[a] Sara Ajmal,[a] Dong Xiang,[a] Zhenjie Sun,[a] Wenxing Chen,[c] Manzhou Zhu,[a,b] Ping Chen,[a] and Peng Li*[a,b]

[a] Department of Chemistry and Centre for Atomic Engineering of Advanced Materials, School of Materials Science and Engineering, Anhui Province Key Laboratory of Chemistry for In-organic/Organic Hybrid Functionalized Materials, Anhui University, Hefei, Anhui 230601, P. R. China.

[b] Key Laboratory of Structure and Functional Regulation of Hybrid Materials, Ministry of Education, Anhui University, Hefei 230601, P. R. China.

[c] Energy & Catalysis Center, School of Materials Science and Engineering, Beijing Institute of Technology, Beijing 100081, China.

* Email: peng-li@ahu.edu.cn (Li P).

Experimental section

Chemical reagents

Sodium Molybdate ($Na_2MoO_4·2H_2O$, 99%), ruthenium oxide (RuO_2 ,99.9%) and dextran-20 (MW=20000) was supplied from Aladdin. Cobalt potassium cyanide ($K_3[Co(CN)_6]$, 99%) was purchased from Picasso (Shanghai) Development Co., Ltd. Nafion (5 wt.%) was bought from Sigma Aldrich. Pt/C (20%) was purchased from Alfa Aesar. Citric acid ($C_6H_5O_7·H_2O$, 99.8%), urea ($CO(NH_2)_2$, 99%), potassium hydroxide (KOH, 85%), hydrochloric acid (HCl, AR) and acetone (CH_3COCH_3, AR) were supplied from Sinopharm Chemical Reagent Co., Ltd.

Synthesis of Mo-NiCo PBA/NF and NiCo PBA/NF

For the Mo-NiCo PBA/NF synthesis, first a piece of NF (1.0 cm × 1.5 cm) was ultrasonically cleaned in dilute hydrochloric acid solution, acetone and deionized water for 15 minutes. 0.1 mmol Dextran-20, and 2.1 mmol $C_6H_5O_7·H_2O$ and 0.05 mmol $Na_2MoO_4·2H_2O$ were dissolved in 300 mL deionized water (Solution A). Then, the mixed solution was added dropwise to 200 mL of a solution that contained 0.5 mmol $K_3[Co(CN)_6]$ (Solution B). The 30 mL mixed solution was transferred to a 40 mL Teflon-lined autoclave with a slice of pretreated NF and kept at 80 ℃ for 10 h to obtain the final Mo-NiCo PBA/NF electrocatalyst. Centrifuge the reacted solution to obtain a Mo-NiCo PBA powder sample. For comparison, a similar processing was used to prepare NiCo PBA/NF without $Na_2MoO_4 \cdot 2H_2O$ in solution A.

Preparation of RuO_2/NF and Pt/C/NF

4.0 mg of RuO_2, 20 μL of Nafion solution (5.0 wt%), and 0.98 mL of ethanol solution were mixed and treated by ultrasonication for 15 minutes to obtain a homogeneous ink, then it was dripped on NF (1.0 cm × 1.5 cm). Finally, RuO_2/NF was obtained after drying. Pt/C/NF was prepared by the same process.

Characterization

The images of scanning electron microscopy (SEM) were recorded by using Hitachi Regulus 8230 with a 15 kV accelerating voltage. The transmission electron microscopy (TEM) and high-angle annular dark-field scanning TEM (HADDF-STEM) characterizations were obtained on a Tecnai TF-20 transmission electron microscope. The powder X-ray diffraction (PXRD) patterns were determined by a Smart Lab 9 KW with Cu Kα radiation. The X-ray photoelectron spectra (XPS) measurements were collected by using a thermal ESCALAB 250. The X-ray absorption spectrum (XAS) was conducted on Table XAFS-500 (Specreation Instruments Co., Ltd., China).

Electrochemical measurements

The electrochemical measurements were conducted in a three-electrode system connected to the CHI 760 E electrochemical workstation. The catalysts self-supported on NF (1.0 cm × 1.5 cm, the actual working area is 1.0 cm × 1.0 cm) were directly used as working electrodes, Hg/HgO electrode was employed as the reference electrode and the Pt sheet electrode was used as the counter electrode. In this work, all potentials were converted into reversible hydrogen electrode (RHE). The Linear Sweep Voltammetry (LSV) curves were performed at a scan rate of 5 $mV \cdot s^{-1}$. All the curves were manually corrected with 95% iR_s compensation (i = catalytic current and R_s = solution resistance). The electrochemical surface areas (ECSAs) can be obtained by measuring the double layer capacitance (Cdl) of the samples. The Cyclic voltammetry (CV) curves were obtained based on the cyclic voltammetry (CV) curves in the non-faradic potential region (0.91 V to 1.01 V vs. RHE) conducted at scan rates from 20 to 100 $mV \cdot s^{-1}$. The urea oxidation reaction (UOR) stability of Mo-NiCo PBA/NF was tested by current-time (i-t) curve at 1.34 V (vs. RHE) for 22 h.

In order to evaluate the usefulness of catalysts, water electrolysis and urea electrolysis were carried out in a two-electrode system using Mo-NiCo PBA/NF as an anode and Pt/C/NF as a cathode. At the same time, RuO_2/NF was used as an anode and Pt/C/NF was used as a cathode for comparison. The electrolyte for the water electrolysis was 1.0 M KOH and the electrolyte for the urea electrolysis was 1.0 M KOH with 0.33 M urea. The electrochemical overall electrolysis test was performed in an H-type electrolytic cell separated by anion-exchange membrane. The urea-assisted electrolytic water stability of Mo-NiCo PBA/NF||Pt/C/NF was tested by i-t curve at 1.5 V (vs. RHE) for 60 h.

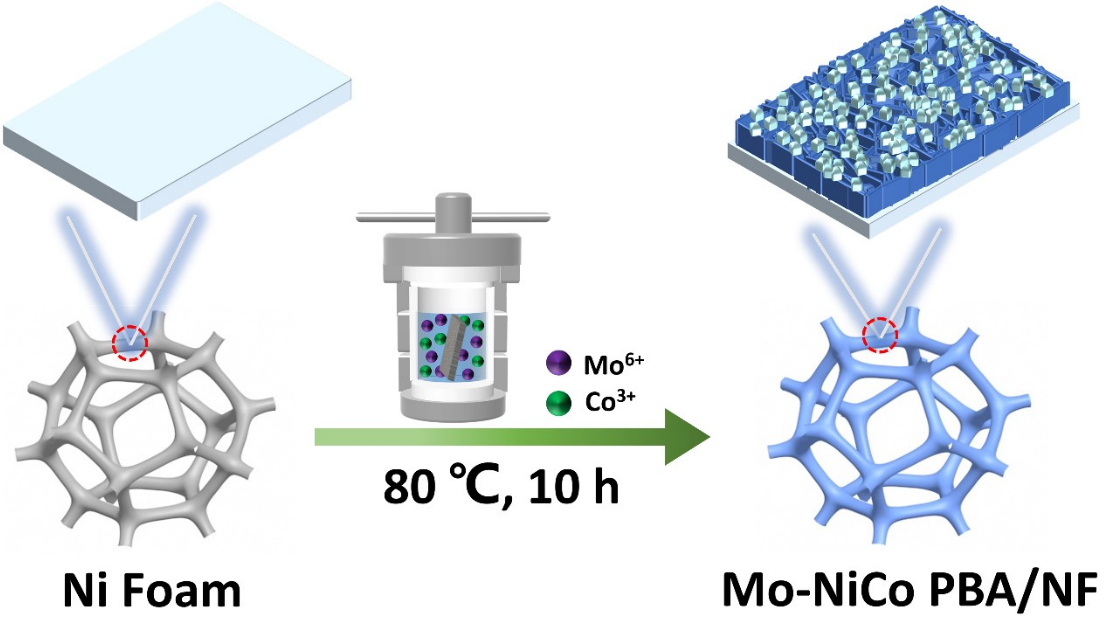

Scheme 1 Schematic illustration for the fabrication of Mo-NiCo PBA/NF.

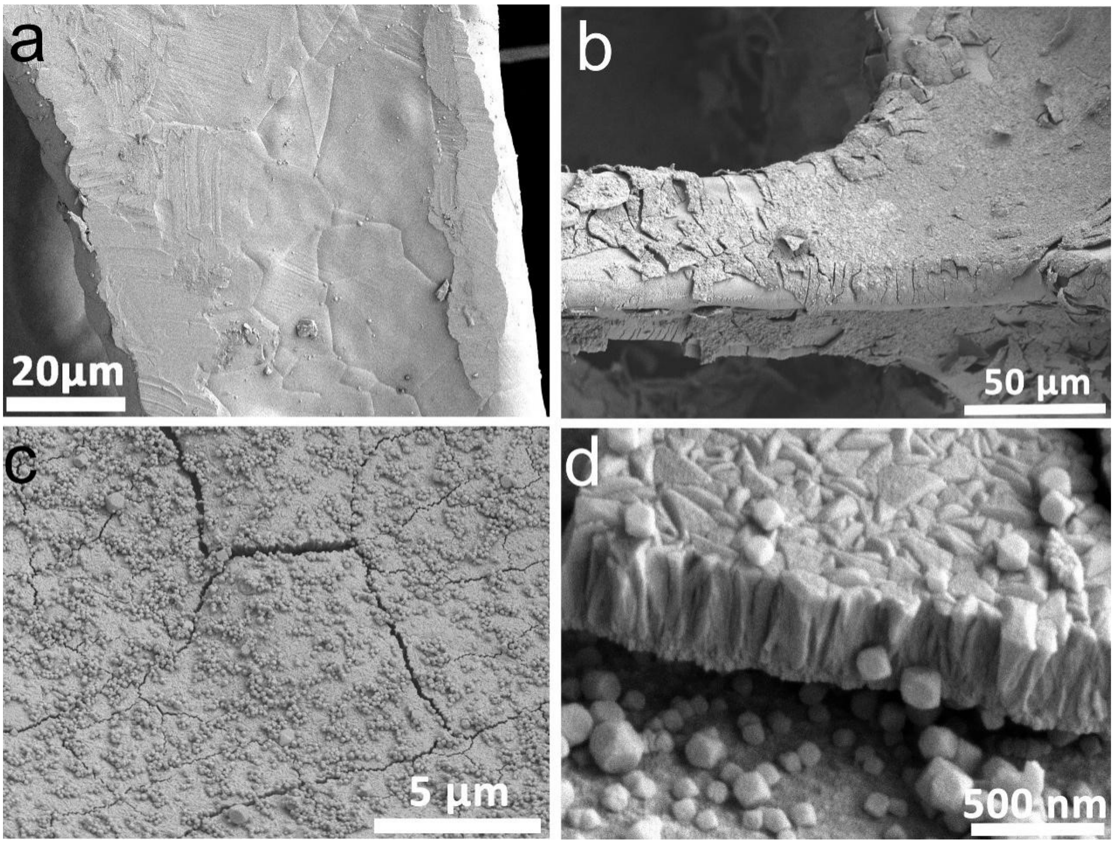

Fig. S1 SEM images. (a) bare NF. (b), (c) and (d) Mo-NiCo PBA/NF.

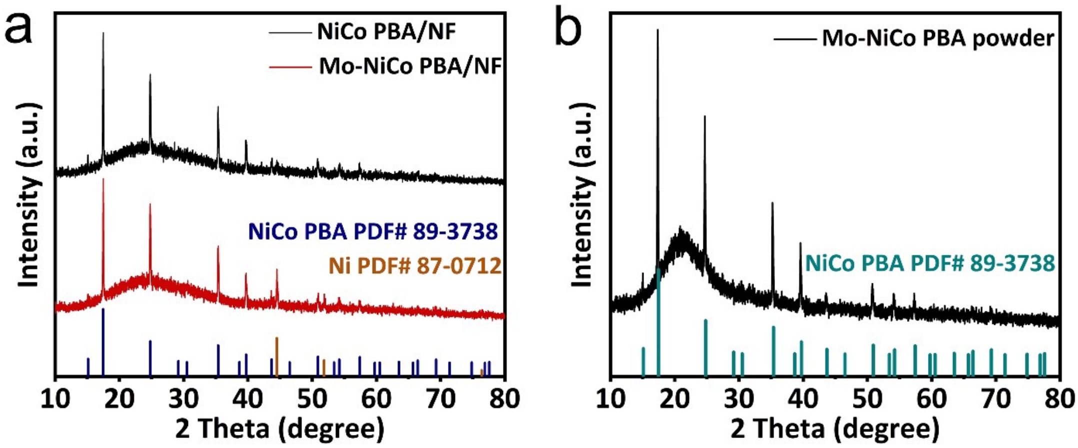

Fig. S2 (a) XRD patterns of Mo-NiCo PBA/NF and NiCo PBA/NF. (b) XRD pattern of Mo-NiCo PBA powder.

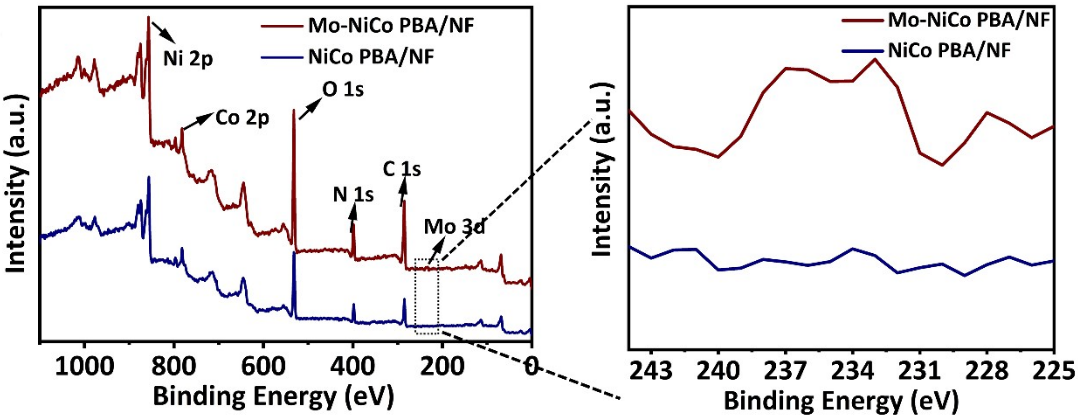

Fig. S3 XPS survey spectra of Mo-NiCo PBA/NF and NiCo PBA/NF.

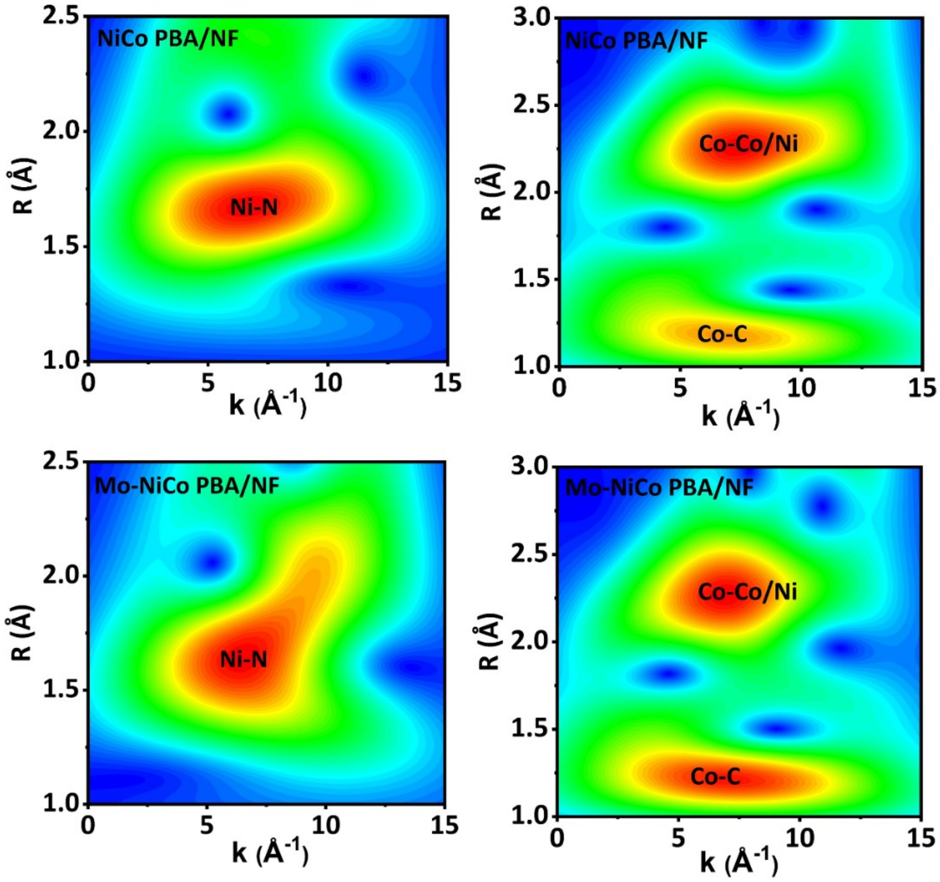

Fig. S4 WT-EXAFS spectra of NiCo PBA/NF and Mo-NiCo PBA/NF.

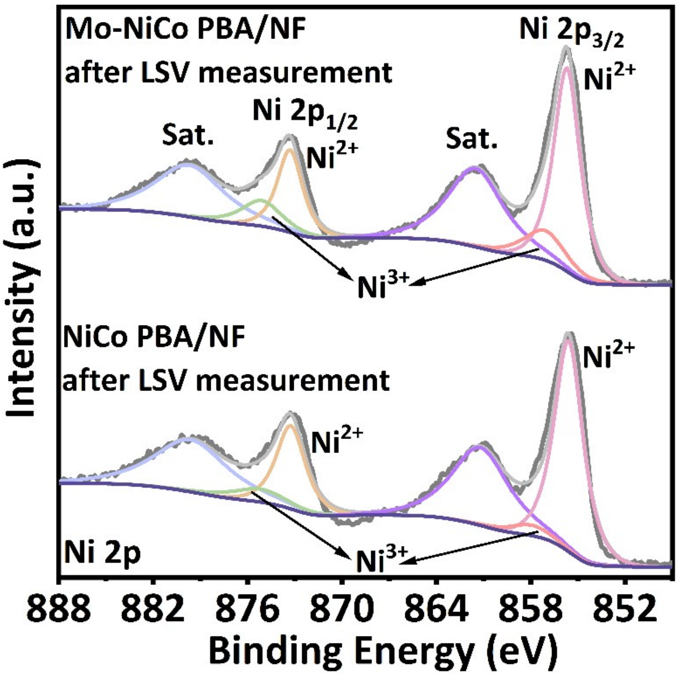

Fig. S5 XPS spectra of Ni 2p of Mo-NiCo PBA/NF and NiCo PBA/NF after LSV measurement of UOR.

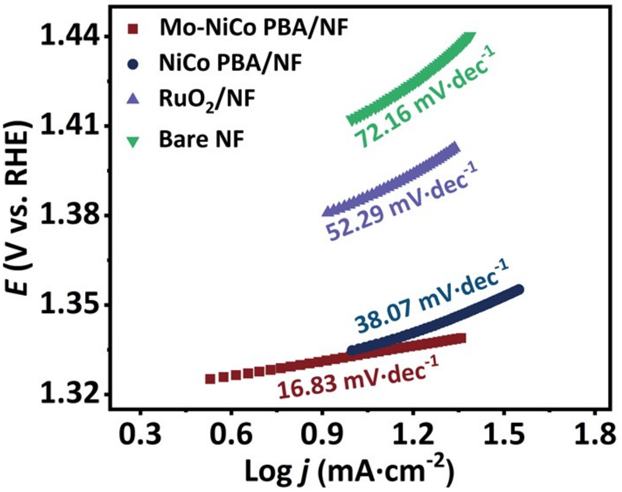

Fig. S6 Tafel slopes of Mo-NiCo PBA/NF, NiCo PBA/NF, RuO_2/NF and bare NF.

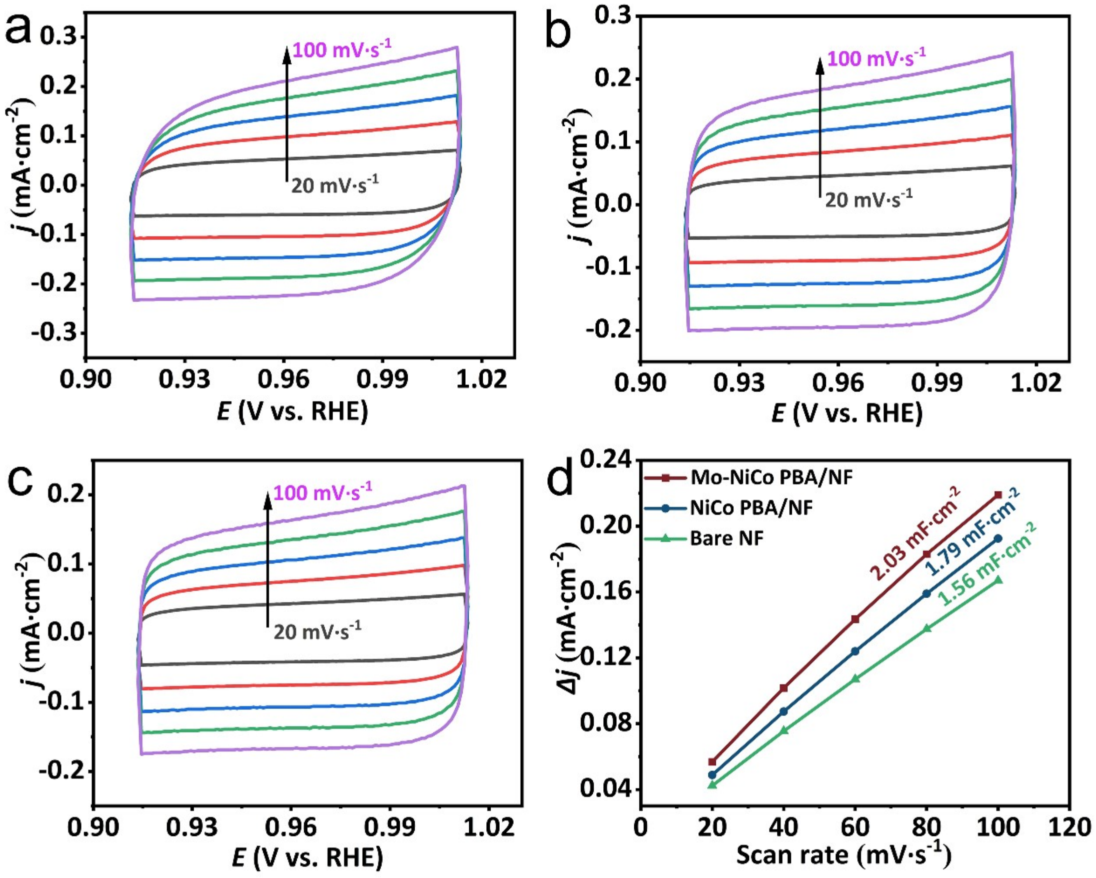

Fig. S7 CV curves of (a) Mo-NiCo PBA/NF, (b) NiCo PBA/NF, and (c) bare NF in the non-faradic potential region (0.91 V to 1.01 V vs. RHE) at various scan rates (20 to 100 mV·s^{-1}). (d) C_{dl} value of the above catalysts.

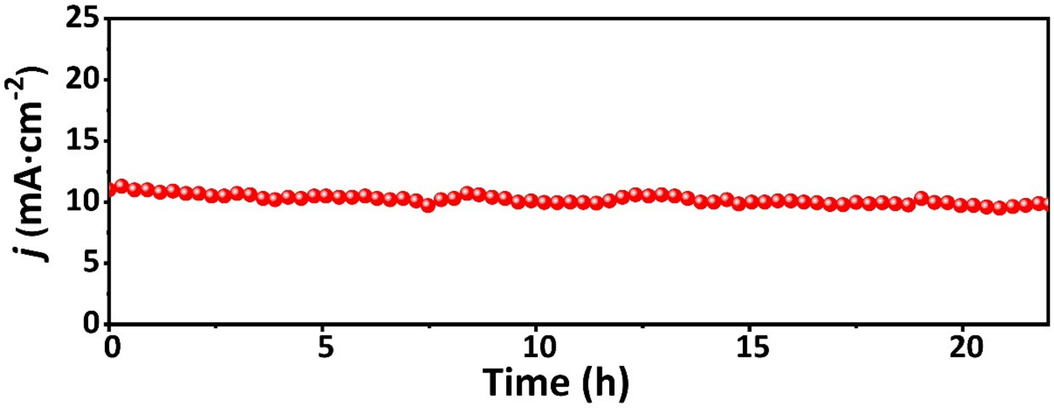

Fig. S8 I-t curve of Mo-NiCo PBA/NF at 1.34 V (vs. RHE) for 22 h.

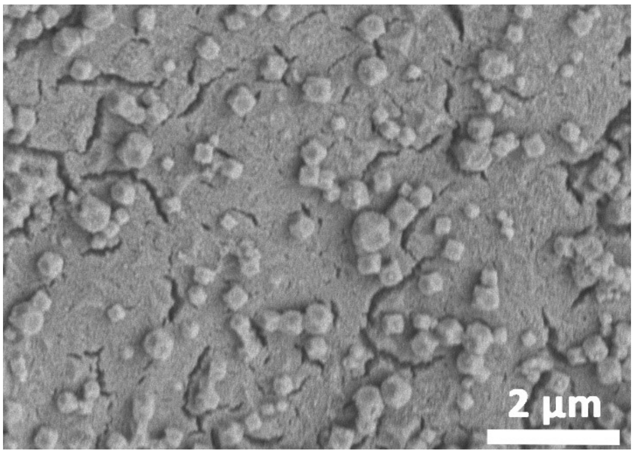

Fig. S9 SEM image of Mo-NiCo PBA/NF after UOR stability test.

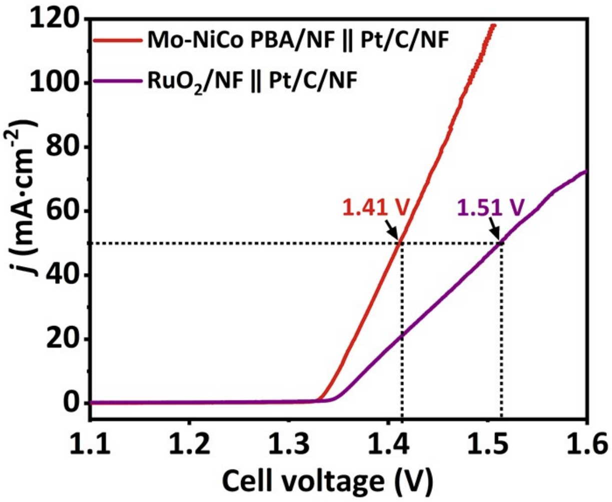

Fig.S10 Polarization curves comparison of Mo-NiCo PBA/NF||Pt/C/NF and RuO$_2$/NF|| Pt/C/NF in 1.0 M KOH with 0.33 M urea.

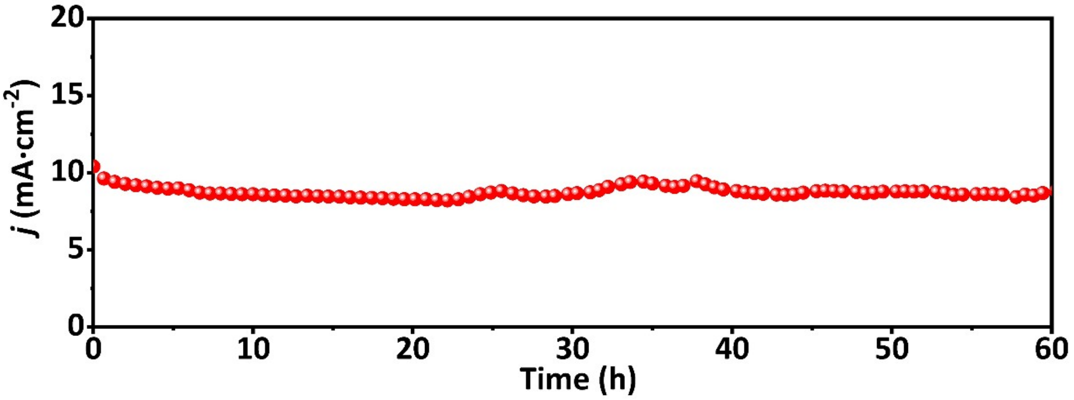

Fig.S11 I-t curve of the Mo-NiCo PBA/NF||Pt/C/NF in 1.0 M KOH + 0.33 M urea at a cell voltage of 1.5 V for 60 h.

Table S1 The atomic% of Mo-NiCo PBA/NF, NiCo PBA/NF, Mo-NiCo PBA powder samples from the EDS analysis.

Element Sample	Ni	Co	Mo
Mo-NiCo PBA/NF	50.00%	47.84%	2.16%
NiCo PBA/NF	55.37%	44.63%	——
Mo-NiCo PBA powder	54.24%	44.70%	1.06%

Table S2 UOR performance comparison between the Mo-NiCo PBA/NF and some other reported electrocatalysts.

Catalysts	Electrolyte	Potential (V vs. RHE) for 100 mA·cm^{-2}	Reference
Mo-NiCo PBA/NF	**1.0 M KOH + 0.33 M urea**	**1.358**	**This work**
NiMoV LDH	1.0 M KOH + 0.33 M urea	1.40	1
O-NiMoP/NF	1.0 M KOH + 0.5 M urea	1.41	2
$NiMoO_4 \cdot xH_2O$/NF	1.0 M KOH + 0.5 M urea	1.36	3
MoP@NiCo-LDH	1.0 M KOH + 0.5 M urea	1.392	4
Co_xMo_yCH	1.0 M KOH + 0.33 M urea	~1.52	5
Mo-doped Ni_3S_2	1.0 M KOH + 0.3 M urea	~1.38	6
Ni-TPA@NiSe/NF	1.0 M KOH + 0.5 M urea	1.37	7
PBA@MOF–Ni/Se	1.0 M KOH + 0.5 M urea	~1.45	8
NCMO–Ar	1.0 M KOH + 0.5 M urea	1.38	9
Ni–Mn–Se	1.0 M KOH + 0.33 M urea	1.437	10

Table S3 The overall urea splitting performance comparison between the Mo-NiCo-PBA/NF and some other reported electrocatalysts.

Catalysts	**Electrolyte**	**Potential (V vs. RHE) for 50 mA·cm^{-2}**	**Reference**
Mo-NiCo PBA/NF ||Pt/C(+/-)	**1.0 M KOH + 0.33 M urea**	**1.41**	**This work**
$Ni_2Fe(CN)_6$||Pt/C(+/-)	1.0 M KOH + 0.33 M urea	~1.45	11
NiFe NSs/NF||Pt/C(+/-)	1.0 M KOH + 0.33 M urea	~1.60	12
Mn-$Ni(OH)_2$ PNAs ||Pt/C(+/-)	1.0 M KOH + 0.5 M urea	1.50	13
Ni-DMAP-2/NF ||Pt/C/NF(+/-)	1.0 M KOH + 0.5 M urea	~1.52	14
$Ni(OH)_2$@NF||Pt/C/NF(+/-)	1.0 M KOH + 0.3 M urea	1.45	15
Ni_2P||Pt mesh (+/-)	1.0 M KOH + 0.5 M urea	~1.77	16
NiS nanotubes||Pt/C(+/-)	1.0 M KOH + 0.33 M urea	~1.69	17
$Ni(OH)_2$/CuO NWs/CF ||Pt/C(+/-)	1.0 M KOH + 0.5 M urea	~1.43	18

1. Z. Wang, W. Liu, J. Bao, Y. Song, X. She, Y. Hua, G. Lv, J. Yuan, H. Li and H. Xu, *Chem. Eng. J.*, 2022, **430**,133100.
2. H. Jiang, M. Sun, S. Wu, B. Huang, C. S. Lee and W. Zhang, *Adv. Funct. Mater.*, 2021, **31**, 2104951.
3. M. Fang, W.-B. Xu, Y. Shen, P. Cao, S. Han, W. Xu, D. Zhu, Y. Lu and W. Liu, *Appl. Catal. A-Gen.*, 2021, **622**,118220.
4. T. Wang, H. Wu, C. Feng, L. Zhang and J. Zhang, *J. Mater. Chem. A*, 2020, **8**, 18106-18116.
5. S. Zheng, H. Qin, X. Cao, T. Wang, W. Lu and L. Jiao, *J. Energy Chem.*, 2022, **70**, 258-265.
6. H. Xu, Y. Liao, Z. Gao, Y. Qing, Y. Wu and L. Xia, *J. Mater. Chem. A*, 2021, **9**, 3418-3426.
7. L. Jin., R. Ji., H. Wan., J. He., P. Gu., H. Lin., Q. Xu. and J. L.u, *ACS Catal.*, 2023, **13**, 837-847.
8. H. Xu, K. Ye, K. Zhu, Y. Gao, J. Yin, J. Yan, G. Wang and D. Cao, *Inorg. Chem. Front.*, 2021, **8**, 2788-2797.
9. X. Liu, H. Qin, G. Wang, Q. Li, Q. Huang, Z. Wen and S. Mao, *J. Mater. Chem. A*, 2022, **10**, 16825-16833.
10. M. Maleki, G. Barati Darband, A. Sabour Rouhaghdam, R. Andaveh and Z. Mohammad

Kazemi, *Chem. Commun.*, 2022, **58**, 3545-3548.

11. S.-K. Geng, Y. Zheng, S.-Q. Li, H. Su, X. Zhao, J. Hu, H.-B. Shu, M. Jaroniec, P. Chen, Q.-H. Liu and S.-Z. Qiao, *Nat. Energy*, 2021, **6**, 904-912.
12. Y. Diao, Y. Liu, G. Hu, Y. Zhao, Y. Qian, H. Wang, Y. Shi and Z. Li, *Biosens. Bioelectron.*, 2022, **211**, 114380.
13. F. Chen, F. Yang, C. Sheng, J. Li, H. Xu, Y. Qing, S. Chen, Y. Wu and X. Lu, *J. Colloid Interf. Sci.*, 2022, **626**, 445-452.
14. H. Jiang, S. Bu, Q. Gao, J. Long, P. Wang, C.-S. Lee and W. Zhang, *Mater. Today Energy*, 2022, **27**, 101024.
15. L. Xia, Y. Liao, Y. Qing, H. Xu, Z. Gao, W. Li and Y. Wu, *ACS Appl. Energy Mater.*, 2020, **3**, 2996-3004.
16. H. Liu, S. Zhu, Z. Cui, Z. Li, S. Wu and Y. Liang, *Nanoscale*, 2021, **13**, 1759-1769.
17. M. Zhong, W. Li, C. Wang and X. Lu, *Appl. Surf. Sci.*, 2022, **575**,151708.
18. H. Sun, J. Liu, G. Chen, H. Kim, S. Kim, Z. Hu, J. M. Chen, S. C. Haw, F. Ciucci and W. Jung, *Small Methods*, 2022, **6**, 2101017.